THERMOPHYSICAL MODELING OF (15) EUNOMIA FROM HIGH-RESOLUTION ALMA DATA Y. Phua[1], K. de Kleer[1], S. Cambioni[2] [1]Division of Geological and Planetary Sciences, California Institute of Technology, Pasadena, CA, USA [2]Department of Earth, Atmospheric and Planetary Sciences, Massachusetts Institute of Technology, Cambridge, MA, USA (yphua@caltech.edu)

Introduction: Studies of thermal emission of asteroids can provide information about the regolith properties and composition, from which we can infer the nature and evolutionary processes occurring on the underlying body. Thermally emitted fluxes can be detected from infrared radio wavelengths, but are most often studied in the thermal infrared wavelengths [1, 2]. However, it is not possible to obtain spatially resolved observations of asteroids at thermal infrared wavelengths from ground-based or spaced-based telescopes existing today. In contrast, radio interferometry from the Atacama Large Millimeter/submillimeter Array (ALMA) allows for spatially resolving main-belt asteroids at millimeter wavelengths and explore potential spatial variations in thermal properties across the surfaces of asteroids [3].

In this work, we have applied a thermophysical model to 1.3 mm thermal emission data acquired in 2019 with ALMA to derive the best-fit global values of thermal inertia and millimeter emissivity of asteroid (15) Eunomia. Eunomia is the largest stony (S-type) asteroid with a mean diameter of 270 km, which is large enough for ALMA to resolve the surface at 33 km spatial resolution. Past work has inferred both Fe-rich olivine-dominated and pyroxene-dominated regions on its surface. This compositional dichotomy suggests that Eunomia is partially differentiated [4, 5]. Studying the spatial variations in thermal properties across the surface of Eunomia is valuable for understanding the extent of differentiation, which can provide further insights into the formation and evolution of not only Eunomia but of large S-type asteroids more broadly.

Methods: *Observations:* Eunomia was observed with ALMA on 2019 June 13 between 08:59 and 12:06 UTC. The dataset covers half of Eunomia's rotational period with a time resolution of ~5 minutes. The angular resolution was 0.03", corresponding to a resolution of 33 km at Eunomia, which was at a distance of 2.51 AU from the Sun and 1.83 AU from Earth at the time of observation.

Model parameters: We model the observations to determine (1) the thermal inertia, which is a measure of a material's resistance to temperature change over time, and (2) the millimeter emissivity, which is a measure of the dielectric properties of the surface materials. The material properties of bulk surface density and specific heat capacity were fixed at 3500 kg m^{-3} and 367 kg J^{-1} K^{-1} respectively, as in [6]. The thermal skin depth, given by $(P/\pi)^{0.5}\,\Gamma/\rho C$ (P: rotation period, Γ: thermal inertia, ρ: bulk surface density, C: specific heat capacity), was calculated for each thermal inertia value. The electrical skin depth, which sets the depth to which thermal emission is observed from, was initially fixed at 2 mm, as in [6].

Thermophysical model (TPM): To analyze the data, we used a thermophysical model based on [2] and adapted to take into account the spatially resolved thermal emission data including subsurface emission [3, 6]. In our preliminary work, we have assumed a smooth surface. Using the shape model by [7], the TPM by [2] solves the one-dimensional heat conduction equation to output the temperature profile of each asteroid facet as a function of time and depth in the subsurface. As observations at millimeter wavelengths are sensitive to thermal emission from the near-subsurface, our model [3, 6] then integrates the thermal emission through the subsurface to obtain the total emission of each facet. Next, the model maps the model emission images to the same viewing geometry as the spatially resolved ALMA data [3, 6] for direct comparison with the data.

Preliminary results: We have derived the best-fit global values of thermal inertia and millimeter emissivity fitted to the first 12 observations (out of a total of 24 obtained) of Eunomia. As an example, we show the data, model and residuals (data-model) for observation epoch 1 in Fig. 1. Observations 13-24 suffered from deteriorating weather conditions and therefore provide weaker constraints on the model, but will be incorporated as part of future work. The goodness of fit of the models were determined by the χ^2 value:

$$\chi^2 = \sum_{i=1}^{N_{\mathrm{obs}}} \left(\frac{(\mathbf{M}^i - \mathbf{D}^i)}{\sigma_{\mathbf{D}}^i} \right)^2$$

where $\mathbf{M}^i$ is the model and $\mathbf{D}^i$ the observed flux densities of the ith observation, and $\sigma_{\mathbf{D}}^i$ the image background noise of the ith observation (refer to [3, 6] for more details). The results of our thermophysical model of Eunomia indicate a preferred value of emissivity = 0.74-0.76, and thermal inertia = 150-300 J m^{-2} K^{-1} $s^{-0.5}$, although very low thermal inertia values are also permitted with higher values of emissivity (Fig. 1a, b and Fig. 2a).

Figure 1. Data from the observation epoch 1 (left panel), corresponding model images (center panel) and residuals (right panel) for different values of electrical skin depth and thermal inertia, which are: (a) 2 mm, 283, (b) 2 mm, 3, (c) 0.1 mm, 283, (d) 0.1 mm, 3, (e) 2 mm, 283 with a mask applied based on the outline of the data, to match the shape of the model to the shape of the data. The emissivity is 0.74 for (a) and (c)-(e) while the emissivity is 0.90 for (b).

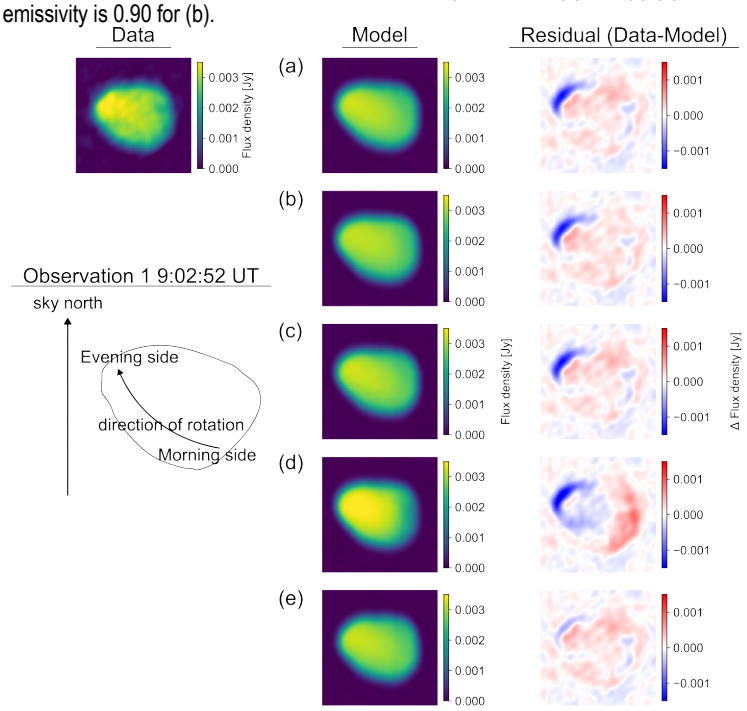

Figure 2. The χ^2 value, which was used to determine the goodness of fit of the model, normalized by the minimum χ^2 value for each combination of thermal inertia and emissivity for (a) electrical skin depth = 2 mm, (b) electrical skin depth = 0.1 mm.

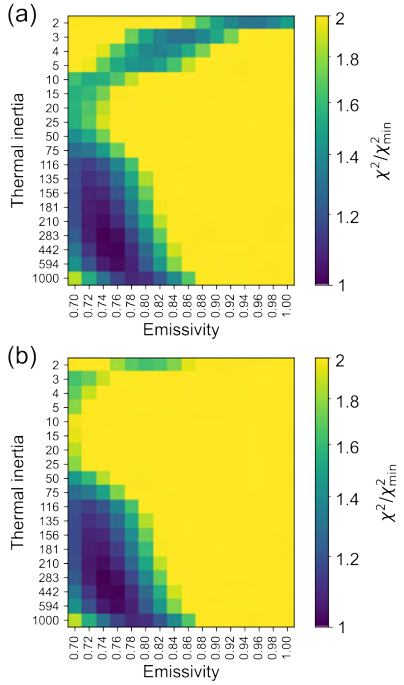

Discussion: Fig. 1a shows a comparison between the observed image and the best-fit model for an electrical skin depth of 2 mm, indicating that the high brightness at the evening side of the asteroid is not well matched by the model. To explore this, we first varied the electrical skin depths to values of 0.1 mm, 0.5 mm, and 1 mm to allow the model to access the warmer nearer-surface temperatures. However, similar values of goodness of fit are achieved with smaller electrical skin depths, emissivity = 0.74-0.76, and thermal inertia = 150-300 J m^{-2} K^{-1} $s^{-0.5}$ (Fig. 2b for electrical skin depth = 0.1 mm; Fig. 1c for residuals of thermal inertia = 283 J m^{-2} K^{-1} $s^{-0.5}$ and electrical skin depth = 0.1 mm). The overall residuals indicate that low thermal inertia values at small electrical skin depths are qualitatively not well fitted to the observed data (Fig. 1d).

The evening edge of the asteroid being brighter in the observed image than the model for an electrical skin depth of 2 mm could be due in part to a mismatch between the observational data and the shape model used to create the model images. Creating a mask based on the observational data and applying it to the model led to some reduction in the residual (Fig. 1e). Using an updated shape model that more accurately represents the asteroid as observed by ALMA will be done in the future. Finally, the mismatch could be also explained by differences in the materials properties across the asteroid, consistent with analysis of previously collected disk-integrated spectra by [4, 5]. Hence future work will focus on fitting the thermal inertia and millimeter emissivity area-by-area, to understand potential spatial variations in thermal properties across the surface of Eunomia.

Our finding that both low and high values of thermal inertia are good fits to the data provide insights into how thermophysics works at ALMA wavelengths. At low thermal inertia values, the thermal skin depth can be much smaller than the electrical skin depth, which was assumed to be a constant of 2 mm. In such a case, the cold deep subsurface is observed, where the diurnal temperature variations are small and the emission therefore mimics that of a higher thermal inertia surface (Fig. 1a, b).

References: [1] Lovell, AJ (2008) *Astrophys. Space Sci.* **313**, 191–196. [2] Delbo, M et al. (2015) *Asteroids IV* 107–128. [3] Cambioni, S et al. (2022) *JGR Planets* **127**, e2021JE007091. [4] Reed, KL et al. (1997) *Icarus* **125**, 446–454. [5] Nathues, A et al. (2005) *Icarus* **175**, 452–463. [6] de Kleer, K et al. (2021) *Planet. Sci. J.* **2**, 149. [7] Vernazza, P et al. (2021) *Astron. Astrophys.* **654**, A56.